

## Alumina phase transformation behavior on titania-doped nano $\alpha$ -alumina by a solid liquid process

Rifki Septawendar<sup>a,\*</sup>, Soewanto Rahardjo<sup>a</sup>, Suhanda<sup>a</sup> and Wisnu Hardik Pratomo<sup>b</sup>

<sup>a</sup>Researchers at Department of Advanced Ceramic, Glass, and Enamel, Center for Ceramics, Ministry of Industry of Indonesia, Akhmad Yani No. 392, Bandung 40272, West Java, Indonesia

<sup>b</sup>Department of Chemistry, University of Padjadjaran, Indonesia

Alumina phase transformation behavior on titania-doped nano  $\alpha$ - $\text{Al}_2\text{O}_3$  powder by a solid liquid process was investigated under various conditions, such as different solvent concentrations and calcining temperatures. Three batches of the precursor powders were calcined at three different temperatures of 600 °C, 750 °C and 900 °C for 5 h and a final product of titania-doped nano  $\alpha$ - $\text{Al}_2\text{O}_3$  powder was obtained. The product has been identified by X-ray diffraction (XRD), scanning electron microscopy (SEM), and transmission electron microscopy (TEM). The XRD results show that the alumina phases of the powders were determined to be  $\gamma$ - $\text{Al}_2\text{O}_3$  and  $\alpha$ - $\text{Al}_2\text{O}_3$ . The optimum calcination temperature of the precursor powder for crystallization of nano  $\alpha$ - $\text{Al}_2\text{O}_3$  was found to be 900 °C for 5 h. A higher concentration of solvent used for the sample preparation leads to the formation of a uniform and very smooth particle morphology, and smaller particle grains. The TEM images indicate that the average size of  $\alpha$ - $\text{Al}_2\text{O}_3$  grains was  $\leq 50$  nm and larger grains of  $\text{TiO}_2$  with 50–250 nm sizes.

**Key words:** Alumina, Phase transformation, Titania, Doping, Calcining temperature, Solvent concentration.

### Introduction

Alumina ( $\text{Al}_2\text{O}_3$ ) shows excellent physical and chemical properties, such as the highest strength among oxides, excellent abrasion resistance, heat resistance, high dielectric strength at high voltage, and high resistance to chemical attack [1]. Therefore, these characteristics have led to the wide use of  $\text{Al}_2\text{O}_3$  in many applications as presented in Table 1.

The applications demand a particular nano-sized powder, so that nano-sized alumina powders will be indispensable for the manufacturing of various advanced materials and devices in the future [3]. The synthesis and control of

materials in nanometre dimensions can access new material properties and device characteristics in unprecedented ways. Controlled structures, large interfaces, power density and other unique characteristics are examples of the superiority of nano-material properties, so that they can access new and improved properties and functionalities [4–6].

Some methods have been used to synthesize and to prepare nano and submicrometre alumina via a chemical route [7, 8]. Sarikaya and Akinc [9], prepared alumina microshells by calcining the precursor with an emulsion evaporation technique; on the other hand, Lin and Wen [10], used a chemical precipitation method to prepare an alumina precursor via an emulsified boehmite gel with oleic acid. Yu-Chen Lee, *et al.* [3], prepared nanoalumina powder by calcining an emulsion precursor derived from aqueous  $\text{Al}(\text{NO}_3)_3$  solution that was mixed with oleic acid. Bastomi *et al.* [11], synthesized submicrometre  $\alpha$ - $\text{Al}_2\text{O}_3$  using the precursor process method. Pati *et al.* [12], prepared nanocrystalline  $\alpha$ - $\text{Al}_2\text{O}_3$  powder at 1150 °C for 2 h by the pyrolysis of a precursor material prepared by evaporation of an aqueous solution of sucrose with polyvinyl alcohol and a metal nitrate. Peng *et al.* [13], synthesized  $\alpha$ - $\text{Al}_2\text{O}_3$  by combustion synthesis using glycine as a fuel and a nitrate as an oxidizer. Ding *et al.* [14], synthesized  $\alpha$ - $\text{Al}_2\text{O}_3$  at 1250 °C via the reaction:  $2\text{AlCl}_3 + 3\text{CaO} \rightarrow \text{Al}_2\text{O}_3 + 3\text{CaCl}_2$ . Pati *et al.* [15], prepared nanocrystalline  $\alpha$ - $\text{Al}_2\text{O}_3$  powder at 1025 °C by the pyrolysis of a complex compound of aluminum with triethanolamine (TEA) and the final material had particles with a 25 nm in size.

Most of the nano  $\alpha$ - $\text{Al}_2\text{O}_3$  preparation methods mentioned are conducted at a relatively high temperature above

**Table 1.** Alumina functional ceramic and its applications [1, 2]

No.	Function	Application
1	Electronic function	IC-Board, Resistor substrates, Electron tube, and others
2	Optical function	High pressure sodium lamp non-volatile memory window
3	Chemical functions	Temperature sensor, catalytic converter, organic catalyst
4	Mechanical functions	Mechanical seals, ceramic liner
5	Biological function	Artificial teeth, artificial joints, artificial bones

\*Corresponding author:

Tel : +6285624249484

Fax: +6222 7205322

E-mail: rifkiseptawendar@yahoo.com

1000 °C. An alternative economical technique to reduce the  $\alpha$ - $\text{Al}_2\text{O}_3$  crystallization temperature is by incorporating appropriate low-temperature crystallization additives such as titania [16, 17]. Therefore, 3% wt ultra fine titania powders were used as a dopant in this nano  $\alpha$ - $\text{Al}_2\text{O}_3$  preparation.

The objective of this study is to evaluate the alumina phase transformation behavior on titania-doped nano  $\alpha$ - $\text{Al}_2\text{O}_3$  powder by a solid liquid process under various conditions, such as different solvent concentrations and calcining temperatures. The products were evaluated by XRD analysis, SEM, and TEM. The scope of this study is limited, and it seems further experimentation and evaluation are necessary for a full understanding.

## Experimental Procedures

Materials used in this research were  $\text{Al}(\text{NO}_3)_3 \cdot 9\text{H}_2\text{O}$ , ultra fine titania powders, 5 M ammonia solution, and technical grade sucrose. All materials were obtained from Merck Inc. Germany; whereas instruments used were a pot mill, a Heraus electrical furnace, a Phillips X-Ray PANalytical, a JEOL JSM-35C SEM, and a JEOL TEM.

## Methods

### Preparation of titania-doped nano $\alpha$ - $\text{Al}_2\text{O}_3$

$\text{TiO}_2$ -doped nano  $\alpha$ - $\text{Al}_2\text{O}_3$  precursors were obtained by mixing 3% (w/w) ultra fine  $\text{TiO}_2$  powders and 97% (w/w) aluminum nitrate in three different solvent concentrations (100 ml (A), 150 ml (B), 200 ml (C)) and milling the mixtures for 90 minutes. About 10% (w/w) sucrose was added appropriately into the mixture and milled until evenly mixed with the mixture. Five molar ammonia solution was added appropriately to the mixture, milled constantly to give an  $\text{Al}(\text{OH})_3$  gel, and heated slowly until a brownish concentrated gel was formed. The gel was then dried in an oven at 200 °C to produce black charcoal precursors. The precursors were milled in a non polar solvent for 24 hours and successfully calcined at 600 °C, 750 °C, and 900 °C in an electric furnace. The final products were identified using XRD, SEM, and TEM.

### Characterization of titania-doped nano $\alpha$ - $\text{Al}_2\text{O}_3$

The crystalline phase and average crystallite size of calcined powder were determined by X-Ray Powder Diffraction (XRD Merck Phillips PW 3710 mpd control with a Cu target). A scanning electron microscope (SEM, JEOL JSM-35C) and transmission electron microscope (TEM, JEOL) studies were performed to verify the morphology and the grain sizes.

## Results and Discussion

### Alumina phase transformation behavior of titania-doped nano $\alpha$ - $\text{Al}_2\text{O}_3$ based on XRD analysis

Figs. 1-3 show typical XRD patterns of titania-doped nano  $\alpha$ - $\text{Al}_2\text{O}_3$  calcined at the temperatures of 600 °C, 750 °C, and 900 °C, respectively. The XRD analysis

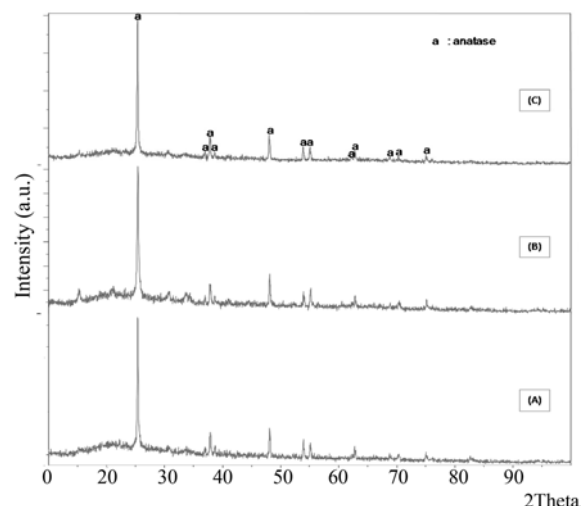


Fig. 1. XRD diffraction patterns of titania-doped nano alumina precursor for all batches namely A (100 ml of solvent), B (150 ml of solvent), C (200 ml of solvent), respectively at 600 °C.

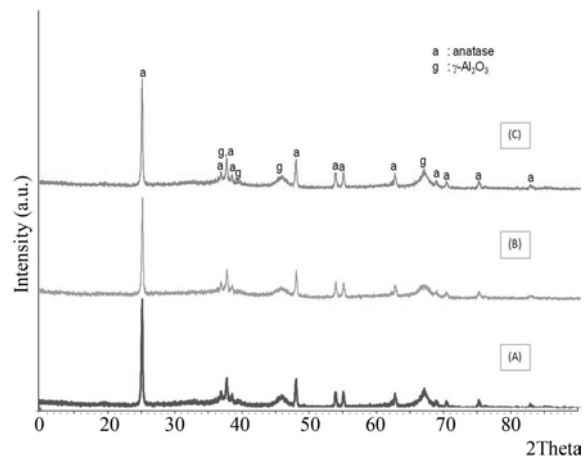


Fig. 2. XRD diffraction patterns of titania-doped nano alumina precursor for all batches namely A (100 ml of solvent), B (150 ml of solvent), C (200 ml of solvent), respectively at 750 °C.

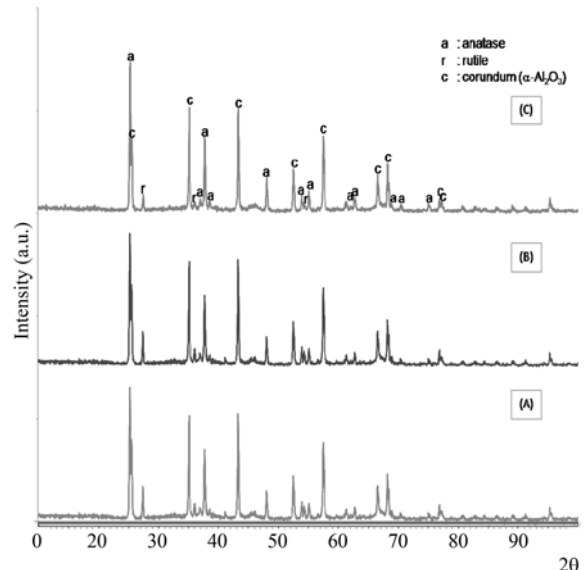


Fig. 3. XRD diffraction patterns of titania-doped nano alumina precursor for all batches namely A (100 ml of solvent), B (150 ml of solvent), C (200 ml of solvent), respectively at 900 °C.

indicates that at a temperature of 600 °C, anatase is the only phase present in all the samples whereas no phases of any alumina transition have been identified in this temperature. At the higher temperature, at 750 °C, the predominant phases in all the samples are anatase, and  $\gamma$ -Al<sub>2</sub>O<sub>3</sub>; and at 900 °C, the phases identified in all the samples are slightly different than at a temperature of 750 °C, where  $\alpha$ -Al<sub>2</sub>O<sub>3</sub>, the most stable alumina phase has been identified with the strong peaks of  $\alpha$ -Al<sub>2</sub>O<sub>3</sub> main crystal planes at diffraction angles of 25.581° [012], 35.156 [104], 43.363 [113], and 57.511 [116]. Therefore, the crystal phase transformation of alumina occurred was  $\gamma$ -Al<sub>2</sub>O<sub>3</sub> (cubic) →  $\alpha$ -alumina (trigonal). According to the result of the XRD analysis, the addition of 3% wt ultra fine titania powder as a dopant on this nano  $\alpha$ -Al<sub>2</sub>O<sub>3</sub> preparation has reduced the crystallization temperature of  $\alpha$ -Al<sub>2</sub>O<sub>3</sub> from above 1000 °C to 900 °C because the normal crystallization temperature of  $\alpha$ -Al<sub>2</sub>O<sub>3</sub> is above 1000 °C [18]. However, the effect of solvent concentrations is not significantly shown in the alumina phase transformation behavior of titania-doped nano  $\alpha$ -Al<sub>2</sub>O<sub>3</sub>.

### **Crystallite sizes of $\alpha$ -Al<sub>2</sub>O<sub>3</sub> based on XRD analysis**

Based on the  $\alpha$ -Al<sub>2</sub>O<sub>3</sub> peaks of XRD patterns from Figs. 1, 2 and 3, the crystallite sizes of  $\alpha$ -Al<sub>2</sub>O<sub>3</sub> for all the samples can be calculated using the Scherrer equation [3, 19]:

$$D = \frac{K\lambda}{\beta \cos\theta} \quad (1)$$

where  $D$  is the crystallite size,  $K$  is a shape factor with a value of 0.9-1.4,  $\lambda$  is the wavelength of the X-rays (1.54056 Å),  $\theta$  is Bragg's angle and  $\beta$  is the value of the *full width at half maximum* (radian). According to the Scherrer equation, the crystallite sizes of three alumina samples were calculated and are presented in Table 2.

### **Effect of solvent concentrations to morphology and particle size characteristic**

According to the SEM micrographs as presented in Fig. 4, the particle sizes of the TiO<sub>2</sub>-doped nano  $\alpha$ -Al<sub>2</sub>O<sub>3</sub> were found to be 50-275 nm at 900 °C. The brighter particles in the SEM micrographs show the titania present on the

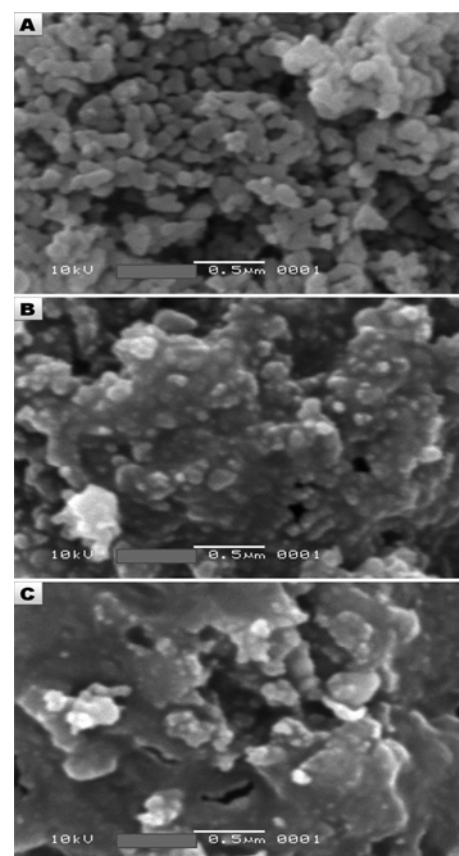


**Fig. 4.** Scanning electron microscope micrographs of TiO<sub>2</sub>-doped nano  $\alpha$ -Al<sub>2</sub>O<sub>3</sub> powders calcined at 900 °C for 5 hours for all batches namely A (100 ml of solvent), B (150 ml of solvent), C (200 ml of solvent), respectively.

powders of TiO<sub>2</sub>-doped nano  $\alpha$ -Al<sub>2</sub>O<sub>3</sub>. The particle sizes of the powders are sensitive to the solvent concentrations in the feedstock for preparation. The effect of the solvent concentration is significantly shown in the particle morphology of titania-doped nano  $\alpha$ -Al<sub>2</sub>O<sub>3</sub>. This is shown by the different SEM micrographs for each sample. A SEM micrograph of a sample using 100 ml of solvent (Fig. 4(A)) shows a homogenous particle morphology and larger grain size of particles, whereas a SEM micrograph of a sample using 150 ml of solvent (Fig. 4(B)) shows a homogenous and smooth particle morphology, and a

**Table 2.** The XRD Identification and Average Crystallite Size of  $\alpha$ -Al<sub>2</sub>O<sub>3</sub> by the Scherrer Method

Samples	Phases			Average Crystallite Size of $\alpha$ -Al <sub>2</sub> O <sub>3</sub> (nm)	PDF 2 No.
	600 °C	750 °C	900 °C		
A	Tetragonal Anatase (TiO <sub>2</sub> )	Tetragonal Anatase (TiO <sub>2</sub> ) Cubic $\gamma$ -Al <sub>2</sub> O <sub>3</sub>	Tetragonal Anatase (TiO <sub>2</sub> ) Tetragonal Rutile (TiO <sub>2</sub> ) Trigonal $\alpha$ -Al <sub>2</sub> O <sub>3</sub>	50.5	
B	Tetragonal Anatase (TiO <sub>2</sub> )	Tetragonal Anatase (TiO <sub>2</sub> ) Cubic $\gamma$ -Al <sub>2</sub> O <sub>3</sub>	Tetragonal Anatase (TiO <sub>2</sub> ) Tetragonal Rutile (TiO <sub>2</sub> ) Trigonal $\alpha$ -Al <sub>2</sub> O <sub>3</sub>	56.5	21-1272 (Anatase) 75-1754 (Rutile) 10-0425 ( $\gamma$ -Al <sub>2</sub> O <sub>3</sub> ) 83-2080 ( $\alpha$ -Al <sub>2</sub> O <sub>3</sub> )
C	Tetragonal Anatase (TiO <sub>2</sub> )	Tetragonal Anatase (TiO <sub>2</sub> ) Cubic $\gamma$ -Al <sub>2</sub> O <sub>3</sub>	Tetragonal Anatase (TiO <sub>2</sub> ) Tetragonal Rutile (TiO <sub>2</sub> ) Trigonal $\alpha$ -Al <sub>2</sub> O <sub>3</sub>	53.1	

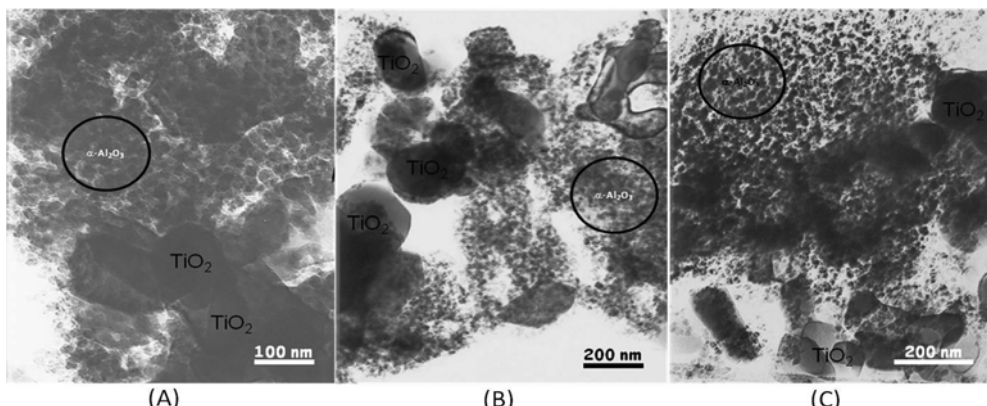


**Fig. 5.** TEM images of  $\text{TiO}_2$ -doped nano  $\alpha\text{-Al}_2\text{O}_3$  powders calcined at  $900^\circ\text{C}$  for 5 hours for all batches namely A (100 ml of solvent), B (150 ml of solvent), C (200 ml of solvent), respectively.

small grain size of particles. Fig. 4(C) shows a SEM micrograph of a sample using 200 ml of solvent in the preparation process, showing a uniform and very smooth particle morphology, and a smaller grain size of particles. The higher concentration of solvent leads to the formation of quite unsaturated  $\text{Al}^{3+}$  ions in the solution, thus the binding distance among them or the particle density will be wider; so that as the calcined temperature increases, the contact among the nucleated  $\alpha\text{-Al}_2\text{O}_3$  grains will occur slowly, leading to the formation of smaller particles.

Typical TEM images of  $\text{TiO}_2$ -doped nano  $\alpha\text{-Al}_2\text{O}_3$  powders for all the samples at  $900^\circ\text{C}$  for 5 h are given in Fig. 5(A)-(C). The images represent small grains of  $\alpha\text{-Al}_2\text{O}_3$  had an average size  $\leq 50$  nm and larger grains of  $\text{TiO}_2$  with 50-250 nm sizes.

## Conclusions

The optimum calcination temperature of the precursor powder for crystallization of nano  $\alpha\text{-Al}_2\text{O}_3$  on a titania-doped nano  $\alpha\text{-Al}_2\text{O}_3$  preparation by a solid liquid process was found to be  $900^\circ\text{C}$  for 5 h.

The effect of solvent concentration is significantly shown in the particle morphology of titania-doped nano  $\alpha\text{-Al}_2\text{O}_3$  powder. A higher concentration of solvent used in the sample preparation leads to the formation of a uniform and very smooth particle morphology, and a smaller grain size of particles as given by SEM.

The TEM results show small grains of  $\alpha\text{-Al}_2\text{O}_3$  had an average size  $\leq 50$  nm and larger grains of  $\text{TiO}_2$  with 50-250 nm sizes.

## References

- Y. Lee, Y.M. Hahn and D.-H. Lee, *J. Ind. Eng. Chem.* 10[5] (2004) 826-833.
- N. Ichinose, K. Komeya, N. Ogino, A. Tsuge and Y. Yokomizo, in "Introduction To Fine Ceramics. Applications In Engineering", (John Wiley & Sons, Inc., 1987)
- Y.-C. Lee, S.-B. Wen and L. Wenglin, *J. Am. Ceram. Soc.* 90[6] (2007) 1723-1727.
- M.C. Roco, in Proceedings of the May 8-9, 1997 Workshop on "R&D Status and Trends in Nanoparticles, Nanostructured Materials, and Nanodevices in the United States", May 8-9, 1997, edited by G.M. Holdridge (Loyola College Press, 1998) 1-3.
- The Royal Society & The Royal Academy of Engineering. Nanoscience and nanotechnologies: opportunities and uncertainties, London, (2004), Retrieved 2008-05-18.
- Guozhong Cao, in "Nanostructures & Nanomaterials: Synthesis, Properties, & Applications" (Imperial College Press, 2004).
- A.K. Bandyopadhyay, in "Nano Materials" (New Age International Press, 2008).
- K.C. Patil, M.S. Hedge, Tanu Rattan and S.T. Aruna, in "Chemistry of Nanocrystalline Oxide Materials, Combustion Synthesis, Properties and Applications" (World Scientific Press, 2008).
- Y. Sarikaya and M. Akinc, *Ceram Int.* 14[4] (1998) 239- 244.
- C.P. Lin and S.B. Wen, *J. Am. Ceram. Soc.* 85[6] (2002) 1467-1472.
- T. Bastomi, B.S. Purwasasmita and R. Septawendar, in Proceeding of Ceramic National Seminar VIII, "The Development of Ceramic Research Result through A Collaboration with Industries To Improve The Competitiveness and The Added Value of The Industrial Products", May 2009, (Center for Ceramics, Indonesia, 2009) 99-104.
- R.K. Pati, J.C. Ray and P. Pramanik, *Materials Letters*. 44[5] (2000) 299-303.
- T. Peng, X. Liu, K. Dai, J. Xiao and H. Song, *Materials Research Bulletin* 41[9] (2006) 1638-1645.
- J. Ding, T. Tsuzuki and P.G. McCormick, *J. Am. Ceram. Soc.* 79[11] (1996) 2956-2958.
- R.K. Pati, J.C. Ray and P. Pramanik, *J. Am. Ceram. Soc.* 84[12] (2004) 2849-2852.
- V.V. Gusarov, Zh. N. Ishutina, A.A. Malkov, A.A. Malygin, O.V. Rybal'chenko and A.P. Shevchik. *Inorganic Materials*, 36[11] (2000) 1127-1932. Translated from *Neorganicheskie Materialy*, 36[11] (2000) 1342-1347.
- C.H. Ting, C. Y. Tan, S. Ramesh and W. D. Teng, *International Conference on Construction and Building Technology*. 18 (2008) 197-202.
- P.S. Santos, H.S. Santos and S.P. Toledo, *Materials Research* 3[4] (2000) 104-114.
- Y.J. Kwon, K.H. Kim, C.S. Lim and K.B. Shim, *J. Ceram. Proc. Res.* 3[3] (2002) 146-149.